New Horizons in Time-Domain Astronomy
Proceedings IAU Symposium No. 285, 2011
R.E.M. Griffin, R.J. Hanisch & R. Seaman, eds.

doi:10.1017/S1743921312000415

Gamma-Ray Waveband and Multi-Waveband Variability of Blazars

Stefano Ciprini[1,2]

[1]ASI Science Data Center, Frascati, Roma, Italy

[2]INAF Observatory of Rome, Monte Porzio Catone, Roma, Italy
email: `stefano.ciprini@asdc.asi.it` (for the Fermi LAT Collaboration)

Abstract. The Fermi Gamma-ray Space Telescope, as an all-sky survey and monitoring mission, is producing well-sampled gamma-ray light curves for dozens of blazars and other high-energy sources. We report highlights of gamma-ray variability properties, and outline multi-frequency observing campaigns that are targeted to new or known blazars which emit gamma rays.

Keywords. surveys, catalogues, gamma rays: observations, quasars: general, BL Lacertae objects: general, methods: statistical, radiation mechanisms: nonthermal

1. Mono- and Multi-Waveband Blazar Variability with Fermi

The Large Area Telescope (LAT), on board the Fermi Gamma-ray Space Telescope (Atwood *et al.* 2009), is a pair-conversion gamma-ray telescope, sensitive to photon energies from about 20 MeV up to >300 GeV, with a wide field of view (> 2.4 sr) and working in all-sky survey mode. The entire sky is observed every 2 orbits (∼3 hours), representing a continuous monitoring of the variable and transient gamma-ray sky and producing regular daily- or weekly-sampled light curves for dozens of GeV sources. Multi-wavelength (MW) observing campaigns are limited only by difficulties in co-ordinating other telescopes. Irregular and aperiodic variability is found in blazars at all the timescales and at all the energies (MW variability). EGRET already showed that blazars have a high-energy component in their spectral energy distributions (SED) and are the largest class of variable gamma-ray sources, although it was limited by statistics, while Fermi is observing low gamma-ray brightness states too. Of the studied Fermi LAT blazars, 2/3 are variable and high states are less than 1/4 of the total light curve range (Abdo *et al.* 2010). Flat Spectrum Radio Quasars (FSRQs) and low energy peaked BL Lac objects (BL Lacs) show the largest relative variance (Fig. 1), while high-energy peaked BL Lacs display a lower variable but persistent emission. Sources like PKS 1510-08, PKS 1502+106 (Fig. 4), 3C 454.3 (Fig. 3; Ackermann et al. 2010), 3C 279 (Fig. 4), PKS 1830-211 (Fig. 2), 4C 21.35, 4C 38.41 (all FSRQs) and AO 0235+164, 3C 66A (both BL Lacs) are among the brightest, most variable, and isotropically luminous blazars seen by Fermi. For bright flares even intra-day light curves have been extracted (Figs. 2 and 3).

Discrete autocorrelation function (DACF) and structure function (SF, Figs. 1 and 3) analysis showed different patterns, autocorrelation times and power-law indices ($1/f^{\alpha}$ trends, where $f = 1/t$) implying different variability modes for each source (more flicker, $\alpha \simeq 1$ or more Brownian, $\alpha \geqslant 2$, dominated). 3C 454.3 is a fully Brownian gamma-ray source while other powerful blazars have values half-way between the two modes. Average power spectral density analysis (PSD) in the frequency domain over the blazar subclasses points out α slopes from 1.3 to 1.6 (Abdo *et al.* 2010; Ackermann *et al.* 2011). No evidence for persistent characteristic gamma-ray timescale(s) is found. Flare profiles are mostly symmetric (in part because of superimposing flares and large bin smoothing).

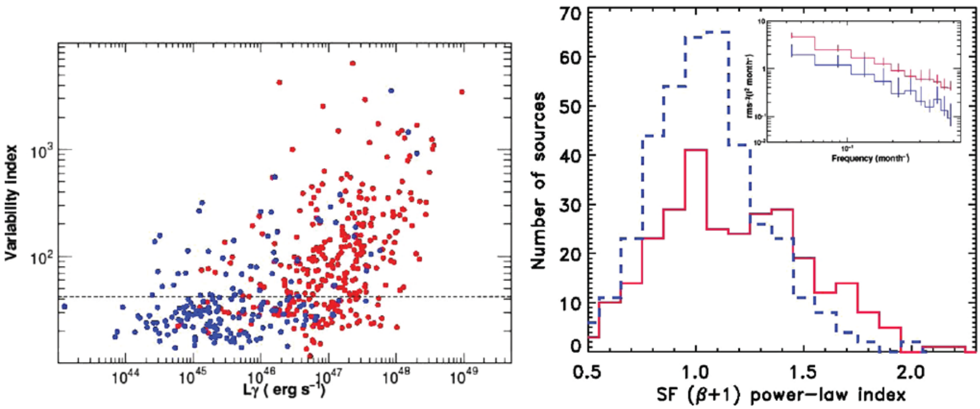

Figure 1. Results from gamma-ray light curves extracted in fixed 1-month bins over the first 2 years of FERMI LAT all-sky survey for the 886 blazars/AGNs of the clean source sample of the second FERMI LAT Source Catalog, 2FGL. Left panel: Variability index versus isotropic gamma-ray luminosity (red/grey: FSRQs; blue/black: BL Lac Objects). Dashed line represents the 99% confidence level for a source to be variable. Right panel: distribution of the temporal power spectral density (PSD) power-law indexes ($\alpha = \beta{+}1$) for the FSRQs (red/continuous line) and BL Lac objects (blue/dashed line) of the sample evaluated in time domain using first-order structure function (SF) analysis (blind power-law index β estimation using a maximum lag of 2/3 of the total light-curve range). Cumulative PSD for bright FSRQs (red/top line) and BL Lac objects sub-samples (blue/bottom line) showing similar slopes (inset). From Ackermann *et al.* (2011).

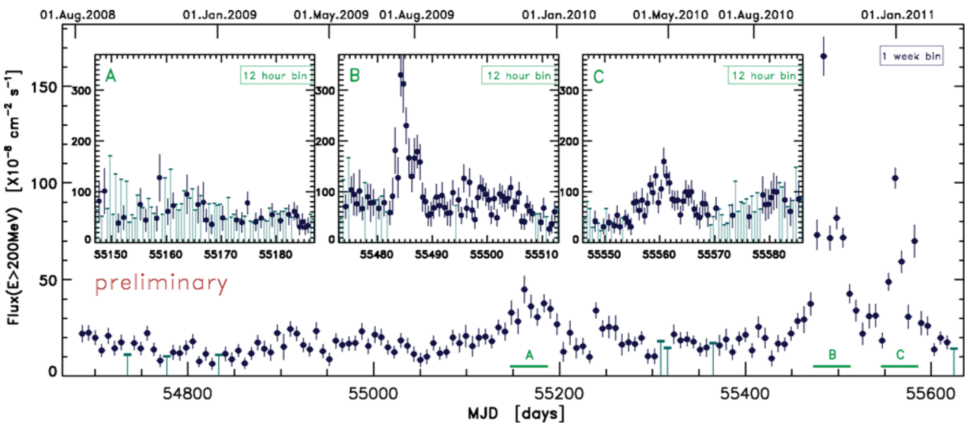

Figure 2. Main panel: 31.5-month (945-day) gamma-ray flux ($E > 200$ MeV) light curve in weekly time bins of blazar PKS 1830-211, from 2008 August 04, to 2011 March 7 (MJD 54682.65 to 55627.65) as an example of the FERMI LAT capabilities in high-energy temporal variability monitoring. Inset panels: 12-hour bin light curves detailing the period around the mild flare of October 2009 (A interval), detailing the period around the large outburst of October 2010 (B interval) and the secondary double flare of December 2010 and January 2011 (C interval).

The fractional variability during outburst appears similar to its longer-term mean in the few objects studied in detail.

FERMI-driven MW observing campaigns are shedding light on the PSD-SED plane (i.e., time-scale–energy parameter space). Broad-band MW studies mostly address cross-correlation and time-lag analysis, model time-resolved SEDs, search for orphan flares and spectral hysteresis and analyse gamma-ray *vs* synchrotron amplitude ratios and emission peaks, and study the radio–gamma-ray connection and source populations. Simultaneous

https://doi.org/10.1017/S1743921312000415 Published online by Cambridge University Press

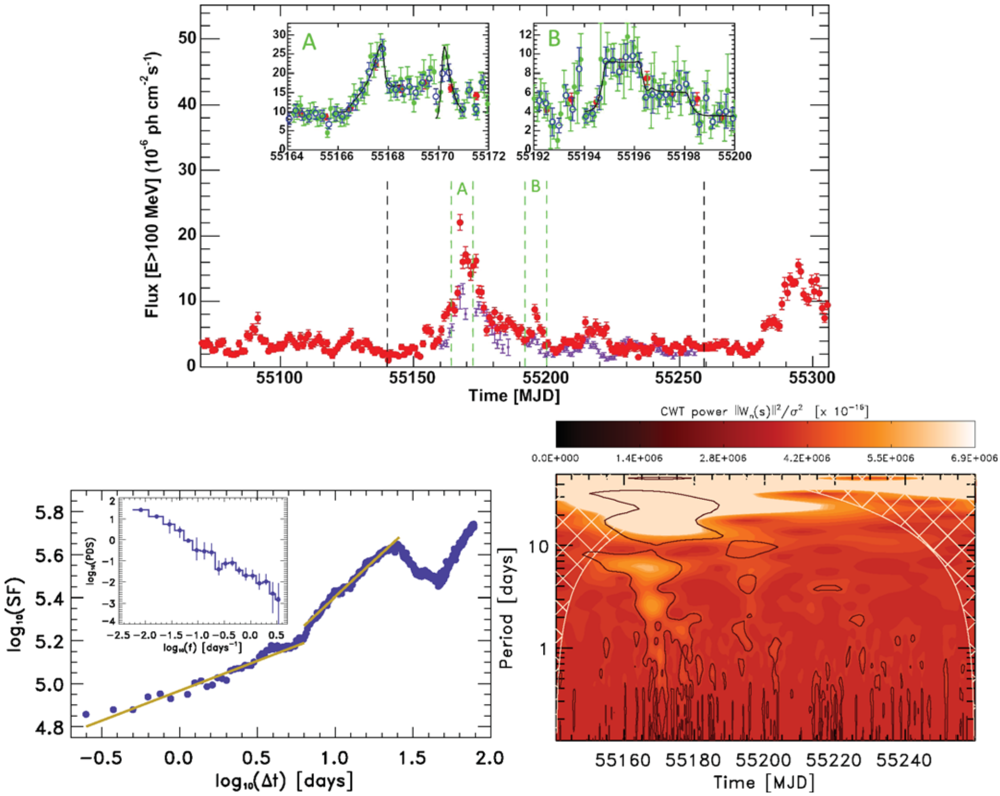

Figure 3. Top panel: daily-bin gamma-ray flux light curve of blazar 3C 454.3 (100 MeV - 200 GeV band, red/gray points, main panel) between 2009 Aug. 27 2010 Apr. 21 (MJD 5507055307). Dashed black lines mark period over which the SF, PSD and Wavelet analysis are conducted (using improved resolution with 3 hour bins). The light curve of the previous 2008 JulyAug. flare, shifted by 511 days, is also shown (violet/dark-grey tiny points). Insets show blow-ups of the two periods (A and B on the plot) when the largest relative flux increases took place (red/gray filled, blue/dark open, green/light-gray filled data points corresponding to daily, 6-hour, 3-hour bin fluxes, respectively). Bottom left panel: SF of the 3h-bin flux light curve for the period 2009 Nov. 5 - 2010 Mar. 4 (MJD 55140-55259, black dashed lines in the top panel) and corresponding PSD (inset). Bottom right panel: plane contour plot of the continuous Morlet wavelet transform power density for the same light curve (thick black contours: 90% confidence levels of true signal features against white/red noise background; cross-hatched region: cone of influence where spurious time-frequency edge effects are important). From Ackermann *et al.* (2010).

MW observations are crucial also for the identification of newly discovered gamma-ray sources.

In order to define and better constrain physical parameters, processes and emission components, to clarify the role of the central engine, jets and their interplay, the jet composition and structure in AGNs and blazars is necessary to collect more different and longer sequences of MW observations. Some clues are already emerging.
(1) The knowledge of redshifts is crucial but ~50% of BL Lacs have still unknown z. (2) Simple single-zone synchrotron self Compton (SSC) descriptions are vanishing. (3) Internal shock models with composite particle energy distributions work well. (4) Cross-correlation analysis with optical polarization provides important clues on jet physics. (5) The location of emission site can be both inside and outside the broad line region (BLR). (6) Magnetic fields are complex but can be highly ordered and jet-aligned during

https://doi.org/10.1017/S1743921312000415 Published online by Cambridge University Press

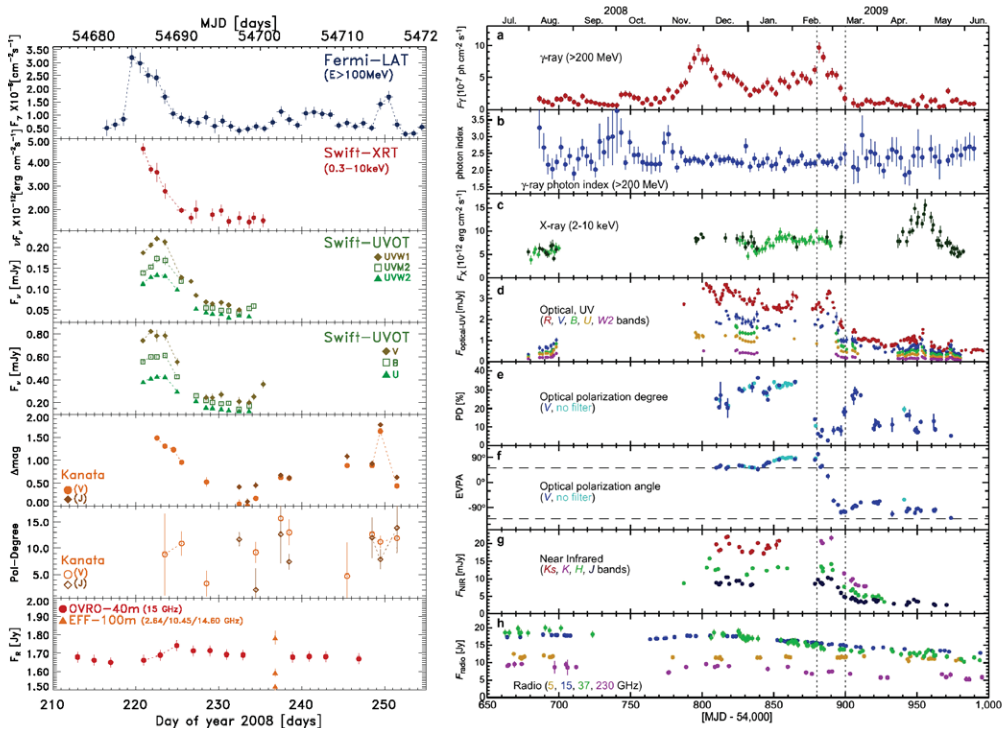

Figure 4. Radio, mm, optical (flux and polarization), UV, X-ray, gamma-ray fluxes light curves obtained by Fermi intensive and coordinated MW campaigns (PKS 1502+106, left, 3C 279, right). From Abdo et al. (2010b,c).

gamma-ray flares. (7) In some cases bright gamma-ray flares seems to occur after ejections of superluminal radio knots. Two examples of composite MW light curves obtained from Fermi blazar campaigns (PKS 1502+106 and 3C 279) are reported in Fig. 4 (Abdo *et al.* 2010b, Abdo *et al.* 2010c). In conclusion, Fermi LAT is demonstrating very good capabilities in the field of gamma-ray variability analysis and radio–gamma-ray connection and is showing an optimal synergy with the Swift mission.

Acknowledgements

The Fermi LAT Collaboration acknowledges support from a number of agencies and institutes for both development and the operation of the LAT as well as scientific data analysis. These include NASA and DOE in the United States, CEA/Irfu and IN2P3/CNRS in France, ASI and INFN in Italy, MEXT, KEK, and JAXA in Japan, and the K.A. Wallenberg Foundation, the Swedish Research Council and the National Space Board in Sweden. Additional support from INAF in Italy and CNES in France for science analysis during the operations phase is also gratefully acknowledged.

References

Abdo, A. A., *et al.* 2010a, *ApJ*, 722, 520
Abdo, A. A., *et al.* 2010b, *ApJ*, 710, 810
Abdo, A. A., *et al.* 2010c, *Nature*, 463, 919
Ackermann, M., *et al.* 2010, *ApJ*, 721, 1383
Ackermann, M., *et al.* 2011, *ApJ*, in press (arXiv:1108.1420)
Atwood, W.B., *et al.* 2009, *ApJ*, 697, 1071